Springer

KSME

Journal of Mechanical Science and Technology 29 (3) (2015) 973~979
www.springerlink.com/content/1738-494x
DOI 10.1007/s12206-015-0211-1

Crane sway reduction using Coriolis force produced by radial spring and damper †

La Duc Viet*

Institute of Mechanics, Vietnam Academy of Science and Technology, 264 Doi Can, Hanoi, Vietnam

(Manuscript Received June 19, 2014; Revised November 10, 2014; Accepted November 17, 2014)

Abstract

This study considers the problem of crane payload sway reduction by spring and damper installed in radial direction between the payload and the cable. Under sway motion, the centrifugal force causes the radial motion, which in turn produces the Coriolis force that reduces sway motion. In free vibration, the non-dimensional analytical form of the optimal spring and damper coefficients can be obtained. Analytical solution shows that the frequency of the radial motion should be twice that of the sway motion. The proposed radial spring and damper exhibits good performance under large sway motions. Numerical simulation of a 2D crane validates the effectiveness of the proposed approach.

Keywords: Coriolis force; Crane anti-sway; Double poles condition; Effective damping; Repeated root condition

1. Introduction

The crane payload suspended by cables is highly flexible. External disturbances, such as wind or the motion of support units (e.g., bridge, trolley, or tower), can cause residual sway oscillation. Over the past two decades, many studies have considered the crane anti-sway control problem. The control strategies proposed in the literature often involve the application of control command to various parts of the crane, such as the cables [1-3], the trolley [4-9], the boom [10, 11], or the active mass damper [12]. The control algorithm can be based on open- or closed-loop techniques. The closed-loop (feedback) techniques use the crane measurements (e.g., deflection, position, etc.) to generate the control command. The feedback control provides disturbance rejection. However, accurate measurements of payload deflection and other system states are not easy to obtain, because the sensors can be expensive as well as difficult to mount, calibrate, and maintain. The feedback control can also cause unexpected motions that could prevent the human operator from driving the crane smoothly. In fact, the human operator is also a feedback controller, and competing feedback controllers can degrade performance [13]. Meanwhile, a typical open-loop technique, that is, input shaping, modifies the desired velocity command before being issued to the crane motors [14-16]. The input shaping techniques are easy to apply and do not require sensors. However, they cannot handle external disturbances or initial conditions. Although many studies on crane open- and closed- loop control can be found in the references of the aforementioned papers, the current paper proposes a more conventional damping system.

The passive damper is the most popular and simple device for vibration control. However, limited studies are available on the application of the passive damper to crane control. The main reason is that the installation of a passive damper into a pendulum with a single cable is hard to imagine. The current paper is motivated by the fact that the radial motion of a mass can produce the Coriolis damping to reduce the sway motion of a pendulum [17-19]. However, this phenomenon only appears in large nonlinear vibrations. Therefore, if the nonlinearity of the pendulum is considered, the opportunity is opened for converting the radial movements between the cables and the payload into the energy dissipation in the dampers. The proposed damping system in the present paper is purely passive and it cannot replace the active control schemes (if any). Instead, because the passive devices do not rely on sensors and external energy, the proposed damping system is expected to improve any active control scheme acting on the crane. Moreover, the proposed system also has other advantages: has good effect in large vibration, minimizes the crane modification, and usable for spherical pendulum.

The rest of this paper is organized as follows. The full nonlinear equation is derived in Sec. 2. In Sec. 3, the second order approximation combined with effective damping approach is used to find the analytical optimal parameters in free vibration. In Sec. 4, the damper effectiveness is demonstrated by performing numerical simulations of the crane payload sway

*Corresponding author. Tel.: +84 945689982, Fax.: +84 437622039
E-mail address: laviet80@yahoo.com, ldviet@imech.ac.vn
† Recommended by Editor Yeon June Kang

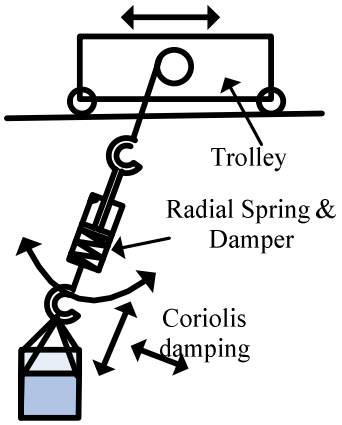

Fig. 1. Concept of radial spring-damper.

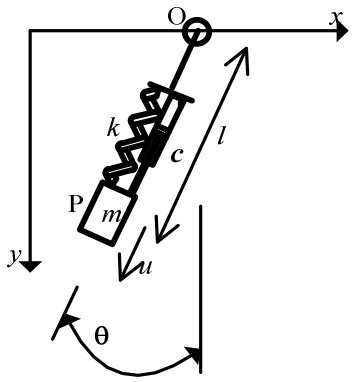

Fig. 2. Symbol used in system modeling.

caused by the motions of support units and by the initial conditions.

2. Problem formulation

The concept of the radial spring-damper for reducing crane sway motion is shown in Fig. 1.

When the payload is in sway motion, the centrifugal force acting on the payload changes with time and the payload is in radial motion. The radial motion in turn produces the Coriolis damping that acts on the sway motion of the payload and reduces it. This approach is effective for large vibrations, because the Coriolis force is a second order term. This proposal has two more advantages: the crane modification is minimal, and the extension in the case of spherical pendulum of 3D crane is visible. The approach based on the radial spring, however, still has a disadvantage as there are strict specifications on the length of the cable. This is an obvious trade-off consequence because a small radial motion is sacrificed to reduce a larger sway motion. As shown in Fig. 1, because the spring and damper are simple connections between the payload and the cable, they can be easily removed in the case of strict requirements of radial movement. Moreover, the radial movement be also reduced by increasing the damping.

To illustrate the nature of the radial spring and damper, some following simplified assumptions have been made:

- Only the 2D crane is considered, i.e. there are two commands: the trolley motion and hoisting commands.
- If the spring and damper weights are ignored in comparison with the payload weight, the single pendulum can be used to model the system. When the spring and damper weights are taken into account, the double pendulum model should also be considered.
- When that cable's stiffness is large enough in comparison with the spring stiffness, the cable deformation can be ignored. In future studies, the effect of the cable's elasticity should be taken into account, especially for a very heavy payload.

With those three simplifications, to write the motion equations, the symbols are shown in Fig. 2, in which, m is the payload weight, k and c respectively are the spring and damper coefficients, l is the distances between the trolley and the payload in the static condition, u is the payload radial motion measured from static position, and θ is the sway angle.

On the coordinate system in Fig. 2, with the horizontal position of the trolley as x, the position of the payload (x_P, y_P) is obtained as

$$x_p = x + (l+u)\sin\theta, y_P = (l+u)\cos\theta . \tag{1}$$

The kinetic energy T, the potential energy V, and the energy dissipation function F are

$$T = \frac{m}{2}\left(\dot{x}_p^2 + \dot{y}_p^2\right); V = \frac{ku^2}{2} + mg\left(l+u-y_P\right); F = \frac{c\dot{u}^2}{2} \tag{2}$$

where g is the acceleration of gravity. The system has 2 degrees of freedom: θ and u. The Lagrange equations are given by

$$\frac{d}{dt}\left(\frac{\partial(T-V)}{\partial\dot{q}}\right) - \frac{\partial(T-V)}{\partial q} + \frac{\partial F}{\partial\dot{q}} = 0 \qquad (q = \theta, u) . \tag{3}$$

Using Eqs. (1), (2) in Eq. (3) gives:

$$\begin{aligned} &2\left(\dot{l}+\dot{u}\right)\dot{\theta} + \cos\theta\ddot{x} + \ddot{\theta}\left(l+u\right) + g\sin\theta = 0 \\ &m\ddot{x}\sin\theta + m\left(\ddot{l}+\ddot{u}\right) + ku + c\dot{u} \\ &\qquad + mg\left(1-\cos\theta\right) - m\dot{\theta}^2\left(l+u\right) = 0 . \end{aligned} \tag{4}$$

3. Optimal parameter for free vibration

This section presents the analytical forms of the spring and damper coefficients in the case of free vibration (x = 0, l = const). To write the equations in non-dimensional forms, some parameters are introduced in Table 1.

Table 1. Symbols used to write the non-dimensional equations.

Symbol	Description
θ_0	Initial angle of free vibration
$\omega_s = \sqrt{g/l}$	Natural frequency of sway motion
$\tau = \omega_s t$	Non-dimensional time with time scale ω_s^{-1}
$\alpha = \sqrt{k/m}/\omega_s$	Ratio between natural frequencies
$\zeta = c/(2m\omega_s)$	Damping ratio of damper
$u_n = u/l$	Non-dimensional form of radial movement

The Eq. (4) becomes:

$$\begin{aligned} &2\dot{u}_n\dot{\theta} + \ddot{\theta}(1+u_n) + \sin\theta = 0 \\ &\ddot{u}_n + \alpha^2 u_n + 2\zeta\dot{u}_n + 1 - \cos\theta - \dot{\theta}^2(1+u_n) = 0 \\ &\theta|_{\tau=0} = \theta_0 \end{aligned} \tag{5}$$

in which the dot operator denotes the differentiation with respect to the normalized time τ. The first term in the first equation of Eq. (5) is the Coriolis damping to reduce the sway motion. This Coriolis damping is proportional to the radial velocity of the payload, which means it only shows effect under large vibration. To obtain the analytical solution, more simplifications are made:

- The trigonometric functions are approximated as:

$$\sin\theta \approx \theta;\ \cos\theta \approx 1 - \theta^2/2 .$$

- The normalized displacement u_n is small in comparison with unity that $1+u_n \approx 1$

The Eq. (5) is simplified as:

$$\begin{aligned} &2\dot{u}_n\dot{\theta} + \ddot{\theta} + \theta = 0 \\ &\ddot{u}_n + \alpha^2 u_n + 2\zeta\dot{u}_n + \theta^2/2 - \dot{\theta}^2 = 0 . \end{aligned} \tag{6}$$

Next, the Coriolis term is replaced by the effective damping:

$$\dot{u}_n\dot{\theta} \approx \zeta_e\dot{\theta} \tag{7}$$

in which the effective damping ζ_e is found by minimizing the following error:

$$\int_0^\infty \left(\dot{u}_n\dot{\theta} - \zeta_e\dot{\theta}\right)^2 d\tau . \tag{8}$$

Setting the derivative of Eq. (8) with respect to ζ_e equal to zero gives:

$$\zeta_e = \int_0^\infty \dot{u}_n\dot{\theta}^2 d\tau \Big/ \int_0^\infty \dot{\theta}^2 d\tau . \tag{9}$$

Using Eq. (7) in Eq. (6) gives the following linear differential equation:

$$\dot{\mathbf{p}} = \mathbf{A}\mathbf{p} \tag{10}$$

where $\mathbf{p}$ is the expanded state vector and $\mathbf{A}$ is the system matrix determined by:

$$\begin{aligned} &\mathbf{p} = \left[\theta \quad \dot{\theta} \quad u_n \quad \dot{u}_n \quad \theta^2 \quad \dot{\theta}^2 \quad \theta\dot{\theta}\right]^T; \\ &\mathbf{p}|_{\tau=0} = \left[\theta_0 \quad 0 \quad 0 \quad 0 \quad \theta_0^2 \quad 0 \quad 0\right]^T; \\ &\mathbf{A} = \begin{bmatrix} \mathbf{A}_1 & \mathbf{0}_{2\times5} \\ \mathbf{0}_{5\times2} & \mathbf{A}_2 \end{bmatrix}, \mathbf{A}_1 = \begin{bmatrix} 0 & 1 \\ -1 & -2\zeta_e \end{bmatrix}, \\ &\mathbf{A}_2 = \begin{bmatrix} 0 & 1 & 0 & 0 & 0 \\ -\alpha^2 & -2\zeta & -1/2 & 1 & 0 \\ 0 & 0 & 0 & 0 & 2 \\ 0 & 0 & 0 & -4\zeta_e & -2 \\ 0 & 0 & -1 & 1 & -2\zeta_e \end{bmatrix} \end{aligned} \tag{11}$$

where $\mathbf{0}_{2\times5}$, $\mathbf{0}_{5\times2}$ denote the zero matrices with appropriate dimensions. The effective damping Eq. (9) is rewritten as:

$$\zeta_e = \int_0^\infty p_4 p_6 d\tau \Big/ \int_0^\infty p_2^2 d\tau . \tag{12}$$

In brief, the simplified equations contain Eqs. (10) and (12). The differential Eq. (10) depends on the effective damping ζ_e while this damping in its turn depends on the state vector as shown in Eq. (12).

There are many ways to optimize the system based on the chosen criteria. In the present paper, the conditions of double poles [20, 21] are considered as the optimal conditions to obtain a closed form of the optimal parameters. Because the parameters α and ζ only appear in the matrix $\mathbf{A}_2$, the characteristic polynomial of $\mathbf{A}_2$ is determined by:

$$P_{A_2}(s) = (s + 2\zeta_e)\left(s^2 + 4\zeta_e s + 4\right)\left(s^2 + 2\zeta s + \alpha^2\right) . \tag{13}$$

The quintic polynomial Eq. (13) has one real root and two pairs of roots of complex conjugate. The repeated roots conditions give:

$$\alpha = 2, \zeta = 2\zeta_e . \tag{14}$$

Substitute Eq. (14) into Eq. (11) and we have the linear system depending on the effective damping ζ_e. The last step is to calculate the effective damping from Eq. (12). It is well known that in the linear system Eq. (10), the infinite integrals of the quadratic form in Eq. (12) can be obtained by solving the Lyapunov matrix equations. A general infinite integral of the quadratic form given:

$$J = \int_0^\infty \mathbf{p}^T\mathbf{Q}\mathbf{p} d\tau \tag{15}$$

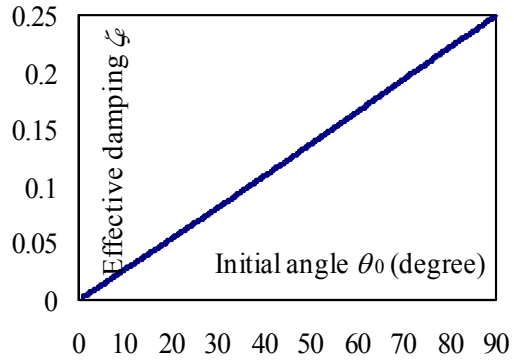

Fig. 3. Effective damping versus initial angle.

where **Q** is a symmetric positive definite matrix. Consider the matrix **P** being the solution of the Lyapunov matrix equation as:

$$\mathbf{PA} + \mathbf{A}^T\mathbf{P} + \mathbf{Q} = \mathbf{0}. \tag{16}$$

Substituting Eq. (16) into the integral Eq. (15) and using the state space Eq. (10) give:

$$\begin{aligned}
&\int_0^\infty \mathbf{p}^T\mathbf{Q}\mathbf{p}d\tau = -\int_0^\infty \mathbf{p}^T\left(\mathbf{PA} + \mathbf{A}^T\mathbf{P}\right)\mathbf{p}d\tau \\
&= -\int_0^\infty \left(\mathbf{p}^T\mathbf{P}\dot{\mathbf{p}} + \dot{\mathbf{p}}^T\mathbf{P}\mathbf{p}\right)d\tau = \left(\mathbf{p}^T\mathbf{P}\mathbf{p}\right)\Big|_\infty^0 \\
&= \mathbf{p}_0^T\mathbf{P}\mathbf{p}_0 - \mathbf{p}(\infty)^T\,\mathbf{P}\mathbf{p}(\infty) = \mathbf{p}_0^T\mathbf{P}\mathbf{p}_0
\end{aligned} \tag{17}$$

in which $\mathbf{p}_0$ is a vector containing the initial conditions and $\mathbf{p}(\infty) = 0$ with the assumption that the system is asymptotically stable due to the presence of damping.

Using Eqs. (16) and (17) in Eq. (12), after some manipulations, we obtain:

$$\zeta_e = \theta_0^2 \frac{3 + 27\zeta_e^2 - 36\zeta_e^4}{128\zeta_e\left(3\zeta_e^2 + 1\right)^2}. \tag{18}$$

The Eq. (18) is a cubic equation of ζ_e^2. In brief, the optimal parameters is obtained by Eqs. (14) and (18). The plot of ζ_e versus θ_0 is shown in Fig. 3.

The effective damping ζ_e is proportional to the initial angle θ_0. This result is from the inherent nonlinearity of the system. In practice, a certain value of θ_0 should be predefined to obtain the optimal parameters.

Formula Eq. (18) is derived for the free vibration case. In other complex operating condition of the crane, it is not easy to develop a clear optimal formula. In the general case, we can modify the Formula Eq. (18) by considering θ_0 as the maximum sway angle when the crane operates.

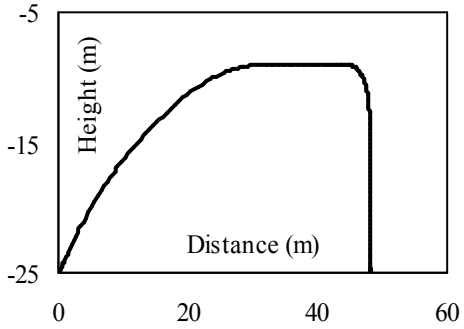

Fig. 4. Trajectory reference.

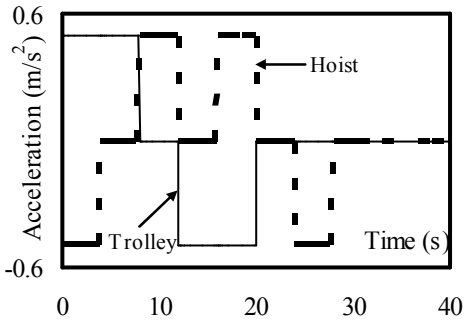

Fig. 5. Commanded accelerations.

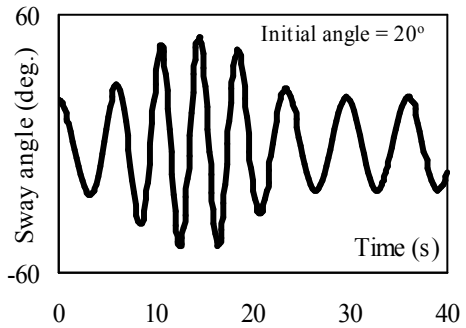

Fig. 6. Sway angle of the cable without spring and damper with the initial angle of 20°.

4. Numerical demonstration

Numerical simulation is performed by solving the full nonlinear Eq. (4). A complex crane motion is simulated. The trolley motion and cable hoisting are combined to move the payload following the predefined trajectory shown in Fig. 4.

The payload is picked up from a point 25 m below the trolley and is raised 16 m with a maximum hoisting velocity of 2 m/s while the trolley moves 48 m simultaneously with a maximum velocity of 4 m/s. The commanded trolley and hoist accelerations are shown in Fig. 5.

To emphasize the effectiveness of the radial spring and damper in reducing free vibration, the initial payload angle is taken into account. The large sway motion occurs when the

Table 2. Optimal parameters for angle of π/3.

Parameter	Value
Optimal frequency ratio α	2
Optimal damping ratio ζ	0.3296
Optimal spring stiffness k	$k = \alpha^2 mg/l = 0.4444mg$
Optimal damper coefficient c	$c = 2m\sqrt{g/l}\zeta = 0.2197m\sqrt{g}$

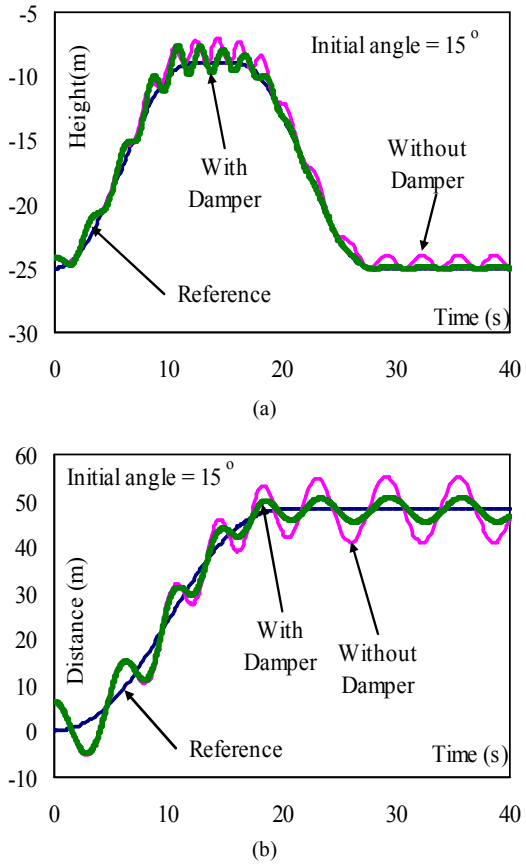

Fig. 7. (a) Payload vertical motion with the initial angle of 15°; (b) payload horizontal motion with the initial angle of 15°.

cable length is short; thus, the spring and damper coefficients are chosen for the minimum cable length, that is, the cable length l in Table 1 is chosen of 9 m. The sway angle of the cable without spring and damper in the case of initial angle of 20° is shown in Fig. 6.

In Fig. 6, the maximum angle is about 60°. Therefore, the damper is designed for the large vibration angle up to 60°, i.e the angle θ_0 is chosen of π/3 in Eq. (18). The results of the optimal parameters are summarized in Table 2.

The payload vertical motions are shown in Figs. 7(a), 8(a), 9(a) and 10(a) for several cases of initial angle. The respective payload horizontal motions are shown in Figs. 7(b), 8(b), 9(b) and 10(b). Two following indices are compared in Table 3

Table 3. Comparisons of error indices.

Initial angle	Index	Without damper	With damper	Reduction
-15°	I_h (m)	3.418	2.201	35.6%
-15°	I_v (m)	0.426	0.276	35.1%
15°	I_h (m)	4.179	2.336	44.1%
15°	I_v (m)	0.656	0.348	47.0%
-20°	I_h (m)	4.638	2.600	43.9%
-20°	I_v (m)	0.791	0.424	46.4%
20°	I_h (m)	5.424	2.769	49.0%
20°	I_v (m)	1.105	0.505	54.3%

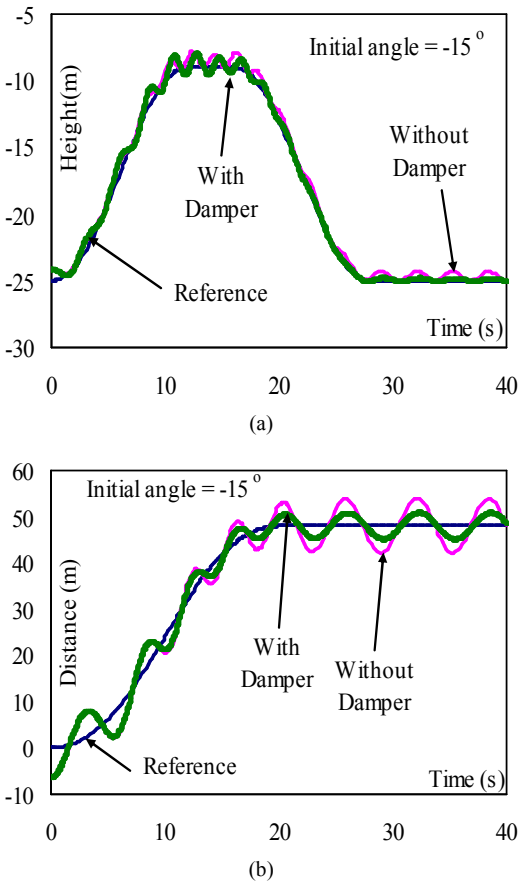

Fig. 8. (a) Payload vertical motion with the initial angle of -15°; (b) payload horizontal motion with the initial angle of -15°.

$$I_h = \frac{1}{T_s}\int_0^{T_s} |x_P - x_r| dt; \qquad I_v = \frac{1}{T_s}\int_0^{T_s} |y_P - y_r| dt$$

where T_s = 40s is the simulation time, x_r and y_r respectively are the horizontal and vertical displacement references as shown in Fig. 4.

The results in the Figs. 7-10 as well as Table 3 clearly show that the proposed radial spring and damper can reduce both the vertical and horizontal errors of the payload movement.

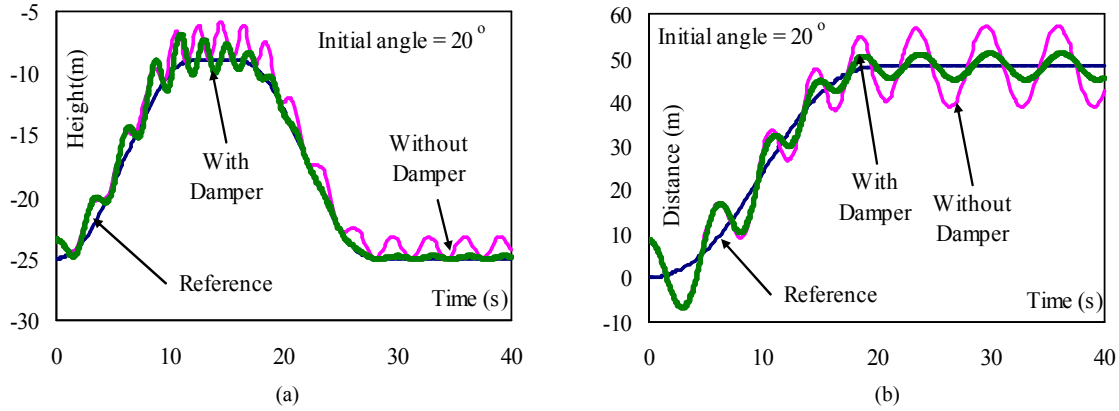

Fig. 9. (a) Payload vertical motion with the initial angle of 20°; (b) payload horizontal motion with the initial angle of 20°.

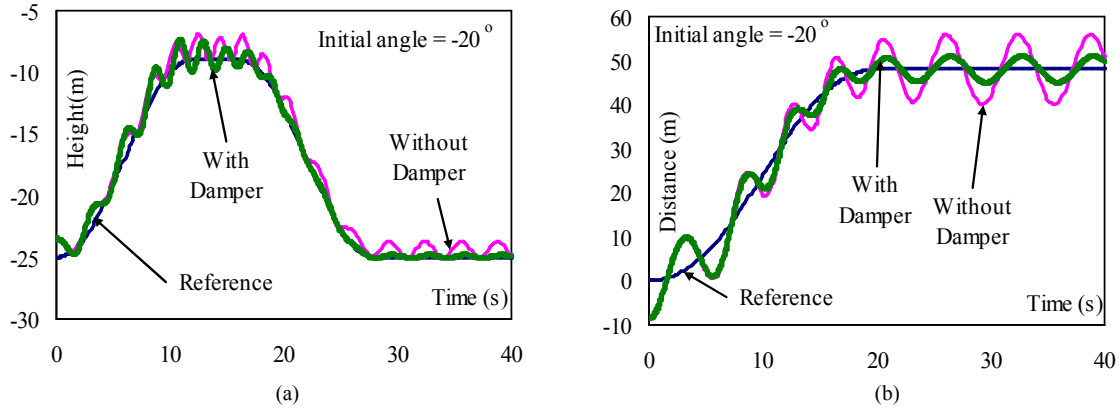

Fig. 10. (a) Payload vertical motion with the initial angle of -20°; (b) payload horizontal motion with the initial angle of -20°.

5. Conclusion

The main objective of this paper is to propose an approach for reducing the crane payload sway motion. The spring and damper are proposed to be installed in the radial direction of the pendulum between the payload and the crane cable. The Coriolis damping is the key factor in the sway motion reduction. The proposed approach has a number of advantages. First, it has a good effect in large vibration that can be considered as a safety device to limit the large sway motion. Second, it minimizes crane modification. Third, it can be used for the spherical pendulum of 3D crane. The analytical optimal parameters are obtained in the case of free vibration. Numerical simulation is performed to verify the conclusions.

Acknowledgment

This research is funded by Vietnam Academy of Science and Technology under grant number “VAST01.09/15-16".

References

[1] N. Q. Hieu and K. S. Hong., Skew control of a quay container crane, *Journal of Mechanical Science and Technology*, 23 (2009) 3332-3339.

[2] D. H. Kim and J. W. Lee, Model-based PID control of a crane spreader by four auxiliary cables, *Proc. IMechE, Part C: J. Mechanical Engineering Science*, 220 (2006) 1151-1165.

[3] Z. Masoud, Oscillation control of quay-side container cranes using cable-length manipulation, *Journal of Dynamic Systems, Measurement, and Control*, 129 (2007) 224-228.

[4] J. H. Suh, J. W. Lee, Y. J. Lee and K. S. Lee, Anti-sway position control of an automated transfer crane based on neural network predictive PID controller, *Journal of Mechanical Science and Technology*, 19 (2) (2005) 505-519.

[5] H. H. Lee, Y. Liang and D. Segura, A sliding-mode antiswing trajectory control for overhead cranes with high-speed load hoisting, *Journal of Dynamic Systems, Measurement, and Control*, 128 (2006) 842-845.

[6] H. C. Cho, J. W. Lee, Y. J. Lee and K. S. Lee, Lyapunov theory based robust control of complicated nonlinear mechanical systems with uncertainty, *Journal of Mechanical Science and Technology*, 22 (11) (2008) 2142-2150.

[7] H. C. Cho and K. S. Lee, Adaptive control and stability analysis of nonlinear crane systems with perturbation, *Journal of Mechanical Science and Technology*, 22 (6) (2008) 1091-1098.

[8] J. Park, O. Kwon and J. H. Park, Anti-sway trajectory generation of incompletely restrained wire-suspended system, *Journal of Mechanical Science and Technology*, 27 (10) (2013) 3171-3176.

[9] L. A. Tuan and S. G. Lee, Sliding mode controls of double-pendulum crane systems, *Journal of Mechanical Science and Technology*, 27 (6) (2013) 1863-1873.

[10] J. Neupert, E. Arnold, K. Schneider and O. Sawodny, Tracking and anti-sway control for boom cranes, *Control Engineering Practice*, 18 (2010) 31-44.

[11] N. Uchiyama, Robust control of rotary crane by partial-state feedback with integrator, *Mechatronics*, 19 (2009) 1294-1302.

[12] H. Kawai, Y. B. Kim and Y. W. Choi, Anti-sway system with image sensor for container cranes, *Journal of Mechanical Science and Technology*, 23 (2009) 2757-2765.

[13] J. Vaughan, E. Maleki and W. Singhose, Advantages of using command shaping over feedback for crane control, *Proc. of American Control Conference*, Baltimore, USA (2010) 2308-2313.

[14] J. Lawrence and W. Singhose, Command shaping slewing motions for tower cranes, *Journal of Vibration and Acoustics*, 132 (2010) 011002.

[15] J. Vaughan, A. Yano and W. Singhose, Comparison of robust input shapers, *Journal of Sound and Vibration*, 315 (2008) 797-815.

[16] D. Blackburn, W. Singhose, J. Kitchen, V. Patrangenaru, J. Lawrence, T. Kamoi and A. Taura, Command shaping for nonlinear crane dynamics, *Journal of Vibration and Control*, 16 (2010) 1-25.

[17] H. Matsuhisa, H. Kitaura, M. Isono, H. Utsuno, J. G. Park and M. Yasuda, A new Coriolis dynamic absorber for reducing the swing of gondola, *Proc. of Asia-Pacific Vibration Conference*, Langkawi, Malaysia (2005) 211-215.

[18] L. D. Viet, N. D. Anh and H. Matsuhisa, The effective damping approach to design a dynamic vibration absorber using Coriolis force, *Journal of Sound and Vibration*, 330 (2011) 1904-1916.

[19] L. D. Viet and Y. J. Park, Vibration control of the axisymmetric spherical pendulum by dynamic vibration absorber moving in radial direction, *Journal of Mechanical Science and Technology*, 25 (7) (2011) 1703-1709.

[20] N. D. Anh, H. Matsuhisa, L. D. Viet and M. Yasuda, Vibration control of an inverted pendulum type structure by passive mass-spring-pendulum dynamic vibration absorber, *Journal of Sound and Vibration*, 307 (2007) 187-201.

[21] S. Krenk, Frequency analysis of the tuned mass damper, *Journal of Applied Mechanics*, 72 (2005) 936-942.

La Duc Viet received his B.S. and Ph.D. degrees in Mechanics from Vietnam National University, Hanoi, Vietnam, in 2002 and 2009, respectively. He is currently a researcher at Institute of Mechanics, Hanoi, Vietnam. His research interests include vibration control, structural dynamics, structural control, and stochastic mechanics.